Carbohydrate Polymers 78 (2009) 760–766

Contents lists available at ScienceDirect

Carbohydrate Polymers

journal homepage: www.elsevier.com/locate/carbpol

A study of the distribution of chitosan onto and within a paper sheet using a fluorescent chitosan derivative

Susana C.M. Fernandes [a], Carmen S.R. Freire [a,*], Armando J.D. Silvestre [a], Carlos Pascoal Neto [a], Alessandro Gandini [a], Jacques Desbriéres [b], Sylvie Blanc [b], Rute A.S. Ferreira [c], Luís D. Carlos [c]

[a] Department of Chemistry and CICECO, Campus de Santiago, University of Aveiro, 3810-193 Aveiro, Portugal
[b] University of Pau and Adour Countries (UPPA), IPREM (UMR CNRS 5254) Helioparc Pau Pyrenées- 2 Avenue P. Angot, 64053 Pau Cedex 09, France
[c] Department of Physics and CICECO, Campus de Santiago, University of Aveiro, 3810-193 Aveiro, Portugal

ARTICLE INFO

Article history:
Received 21 May 2009
Received in revised form 2 June 2009
Accepted 9 June 2009
Available online 16 June 2009

Keywords:
Fluorescent chitosan derivative
Coated paper
Distribution
Luminescence
Reflectance

ABSTRACT

A fluorescent chitosan derivative was deposited layer-by-layer onto conventional paper sheets and its distribution, in terms of both spreading and penetration, was assessed by SEM observations and emission measurements. The results showed that, on the one hand the surface distribution was highly homogeneous and, on the other hand, the penetration of chitosan within the paper pores ceased after a three layer deposit, beyond which any additional coating only produced an increase in its overall thickness and film-forming aptitude. These results show that this modified chitosan can be used as probe to optimize and understand the mechanism of the deposition of chitosan onto paper and other substrates.

1. Introduction

Naturally occurring polymers, such as cellulose, chitin and starch, constitute important renewable sources of novel functional materials, which offer an alternative in response to the economic and depleting problems associated with the use of fossil counterparts. In particular, chitosan (CH), the deacetylated derivative of chitin, has attracted considerable attention in recent years, because of its remarkable properties, which make it particularly suited in such applications as, e.g., biomedical aids, packaging materials and microcapsules for diverse end-uses (Peniche, Argüelles-Monal, & Goycoolea, 2008).

The incorporation of chitosan in paper and paperboard, as a papermaking additive or as a surface coating, has been previously investigated (Bordenave, Grelier, Pichanvant, & Coma, 2007; Gällstedt, Brottman, & Hedenqvist, 2005; Kjellgren, Gällstedt, Engström, & Järnström, 2006; Kuusipalo, Kaunisto, Laine, & Kellomäk, 2005; Li, Du, & Xu, 2004; Vartiainen et al., 2004) and showed that the well-known aptitude of chitosan to form strong thin films could be successfully applied to deposit them onto paper surfaces, thus improving the performance of the ensuing coated materials, in terms of mechanical, gas-barrier, and antimicrobial properties.

Paper materials, including chitosan-coated papers, display a high chemical and morphological heterogeneity, because of the complexity of the interactions among cellulose fibers, fillers and chitosan. Since we felt that these intricacies had not been adequately tackled by previous studies, we decided, within the context of a wider research project on novel chitosan-based materials, to look into this topic in a more systematic fashion, calling upon the use of a fluorescent chitosan derivative as a tool to assess its spatial and in-depth distribution onto the paper sheet. Although fluorescent chitosans have been applied to some biologically related systems (Fang, Ning, Hu, & Lu, 2000; Gåserød, Smidsrød, & Skjåk-Bræk, 1998; Guan, Liu, & Su, 2007; Qaqish & Amiji, 1999; Tømmeraas, Strand, Tian, Kenne, & Vårum, 2001), to the best of our knowledge, they were never reported as additives to paper.

2. Experimental part

2.1. Materials

Chitosan (CH) was kindly provided by the Norwegian Chitosan AS (Norway). Its deacetylation degree (DDA), determined by ^{1}H NMR spectroscopy (in D_2O containing 1% of CD_3COOD) using a DRX-300 Brüker instrument was found to be 90%. Its viscosity-average molecular weight, obtained at 25 °C from a 0.3 M CH_3CO_2H/0.2 M CH_3CO_2Na solution using the published Mark–Houwink constants (Rinaudo, Milas, & Dung, 1993), was 90,000.

* Corresponding author. Tel.: +351 234 370 604; fax: +351 234 370 084.
E-mail address: cfreire@ua.pt (C.S.R. Freire).

0144-8617/$ - see front matter © 2009 Elsevier Ltd. All rights reserved.
doi:10.1016/j.carbpol.2009.06.012

This commercial sample was purified by reprecipitation from a previously filtered 1% aqueous CH_3CO_2H solution into an excess of a 10% NaOH aqueous solution. The ensuing precipitate was extensively washed with distilled water until a neutral pH. The solutions of chitosan and its fluorescent derivative in aqueous CH_3CO_2H used in this study were prepared from this purified sample by stirring for 24 h at room temperature, filtering and degassing. They were thereafter stored in the dark.

The fluorescent chitosan was prepared by the reaction of chitosan with fluorescein isothiocyanate (FITC), following the procedure described by Qaqish and Amiji (Qaqish & Amiji, 1999). A 0.5 mg/mL solution of fluorescein isothiocyanate (FITC, purchased from Sigma–Aldrich, purity 90% minimum) in methanol was slowly added under continuous stirring to a 1% w/v solution of the purified chitosan in 1% v/v aqueous CH_3CO_2H. The condensation between the isothiocyanate groups of FITC and the NH_2 groups of CH was allowed to proceed for 1 h, in the dark, at room temperature. The ensuing FITC–CH derivative was precipitated in a 10% NaOH aqueous solution and washed with distilled water, until the total disappearance of FITC in the washing medium. In order to dispose of a chitosan with a chromophore content which could be visualized and quantified adequately by UV–Vis and luminescence spectroscopy, without altering the actual basic structure of the polysaccharide, only 2.3% of the amino groups of chitosan were modified in this reaction, as determined by elemental analysis.

A3-size papers sheets (100% *Eucalyptus globulus* bleached kraft pulp with a 75 g/m^2 grammage and a 100 μm average thickness, produced by AKD-based sizing system and filled with precipitated calcium carbonate) without any surface treatment, supplied by the Grupo Portucel-Soporcel, Portugal, were used as paper substrates before (control sheets CS) and after coating.

2.2. Coating experiments

The paper sheets were coated with 2% w/v CH or FITC–CH solutions in 1% v/v acetic acid, using a MathisLAB reverse roll coater type RRC-BW 350 mm. In order to achieve different coating weights, five different coating levels were applied using both CH and FITC–CH, with 1 (CH1 or FITC–CH1), 2, 3, 4 or 5 layers on one side of the paper sheet, respectively. The coating speed was fixed at 20 m/min and the distance between the cylinders at 0 mm (adjusting precision ±0.001 mm). The ensuing coated papers were then dried for 2 min at 100 °C in the dryer section of the size press, after each layer deposition. Three replicates were prepared for each condition and each chitosan solution. Thereafter, an A4 sample was cut out from the inner region of each original A3 sheet in order to eliminate the inevitable irregularities associated with its coated borders.

2.3. Characterization of coated paper

Before their characterization, all coated papers were conditioned at 23 ± 1 °C and 50 ± 5% RH for 3 days following the TAPPI T402 om-93 standard. The grammage was determined in accordance with the ISO 536 standard, using a Metter PC 220 analytical balance (±1 mg). The air permeability was measured following the ISO 5636/3:1992 standard using a model 114 Lorentzen & Wettre Bendtsen® Tester. The tensile index was determined using a model 65-F Lorentzen & Wettre Alwetron TH1 tester.

2.4. Evaluation of the distribution of chitosan onto the paper sheets

In all instances, test pieces (4.0 cm × 4.0 cm) were randomly cut off from different regions of the same A4 sheet. These were examined by diffuse reflectance, photoluminescence and scanning electron microscopy (SEM).

The diffuse reflectance spectra of the paper sheets were measured with a Perkin–Elmer 860 Spectrophotometer equipped with a 15 cm diameter integrating sphere bearing the holder in the bottom horizontal position. They were recorded at room temperature in steps of 1 nm, in the range 350–600 nm with a bandwidth of 2 nm. The instrument was calibrated with a certified Spectralon white standard (Labsphere, North Sutton, USA) and spectra were acquired by inserting before the detector a visible short-wave pass filter (LOT-Oriel 450FL07–50, 450 cut-off wavelength) in order to remove the fluorescence component of the chitosan derivative. The reflectance of both sides of the sheet was measured, which provided two spectra for each sample.

The Kubelka–Munk model (Kubelka & Munk, 1931) describes the light penetration in porous media using only two parameters (both with units of cm^{-1}), namely an absorption coefficient, k, and an isotropic scattering coefficient, s. This leads to a very simple relationship between infinite reflectance and absorption and scattering coefficients, known as the remission function, viz.:

$$F(R_\infty) = (1 - R_\infty)^2/2R_\infty = k/s$$

A very important requirement for the use of the Kubelka–Munk model is the homogeneous distribution, both vertically and horizontally, of the absorbed compound in the layer. If the light absorption due to the compound is not excessive, it can be assumed that only the absorption coefficient, but not the scattering coefficient, of the doped medium changes by adding the light-absorbing compound. The absorption coefficient of the system, $k_{tot} = k + k_i$, given by the sum of the absorption coefficient of the medium (k) and that of the compound adsorbed on the solid surface of the medium (k_i), is proportional to the molar absorption coefficient of the compound, $\varepsilon_i(\lambda)$ (cm^3/mol.cm), and to its adsorbed concentration C_i (mol/cm^3).

The photoluminescence spectra were recorded at room temperature with a modular double grating excitation spectrofluorimeter equipped with a TRIAX 320 Fluorolog-3, Jobin Yvon-Spex emission monochromator and coupled to a R928 Hamamatsu photomultiplier, using the front-face acquisition mode. The excitation source was a 450 W Xe arc lamp. The emission spectra were corrected for detection and optical spectral response of the spectrofluorimeter and the excitation spectra were corrected for the spectral distribution of the lamp intensity using a photodiode reference detector.

The radiance measurements and the CIE (x,y) emission colour coordinates were performed using a TOP 100 DTS140–111, Instrument Systems telescope optical probe. The excitation source was a Xe arc lamp (150 W) coupled to a TRIAX 180 Jobin Yvon-Spex monochromator. The width of the rectangular excitation spot was set to 2 mm and the diameter used to collect the emission intensity to 0.5 mm. The emission colour coordinates and the radiance of an uncoated paper were also measured. For all the measurements, the experimental conditions (excitation and detection optical alignment) were kept constant to enable the quantitative comparison between the measurements to be carried out. A mapping of the radiance and colour coordinates was performed using 12 paper pieces (4.0 cm × 4.0 cm) cut off from different regions of the same A4 sheet and 20 measurements were conducted for each sample and their the average value is reported here. The experimental error was within 10%.

For the SEM observation, control sheet and chitosan-coated test pieces were placed, in front and sideway positions so as to visualize both their surface and cross-section. After the carbon coating procedure, the samples were analyzed using an ultra-high resolution analytical scanning electron microscope HR-FESEM Hitachi SU-70, operating at 1.5 kV.

Table 1
Grammage gain and Bendtsen air permeability of CH-coated papers and FITC–CH-coated papers.

Grammage gain [g/m^2]						
	CS	1 layer	2 layers	3 layers	4 layers	5 layers
CH	–	1.5 ± 0.18	2.5 ± 0.2	3.2 ± 0.28	3.9 ± 0.15	4.6 ± 0.30
FITC–CH		1.5 ± 0.04	2.6 ± 0.34	3.3 ± 0.23	4.1 ± 0.165	4.9 ± 0.37
Bendtsen Air Permeability [m/Pa.s]						
CH	9.6 ± 0.28	8.0 ± 0.18	3.3 ± 0.17	0.8 ± 0.07	0.2 ± 0.02	0.0 ± 0.00
FITC–CH		8.1 ± 0.12	3.5 ± 0.05	0.9 ± 0.04	0.2 ± 0.02	0.0 ± 0.00

Table 2
Tensile Index of CS, CH-coated paper and FITC–CH-coated paper in machine direction (MD) and cross direction (CD).

Tensile Index [N.m/g]						
	CS	CH1	CH2	CH3	CH4	CH5
MD	88.4 ± 1.1	100 ± 1.2	110 ± 1.2	114 ± 0.3	115 ± 0.7	117 ± 0.8
CD	26.0 ± 0.4	28.7 ± 0.4	31.8 ± 1.0	34.0 ± 1.8	35.3 ± 0.7	37.5 ± 0.4
	CS	FITC–CH1	FITC–CH2	FITC–CH3	FITC–CH4	FITC–CH5
MD	88.4 ± 1.1	99.7 ± 1.0	105 ± 0.6	110 ± 0.9	113 ± 0.5	114 ± 0.7
CD	26.0 ± 0.4	29.1 ± 0.8	32.9 ± 0.6	34.4 ± 1.1	35.9 ± 0.4	38.7 ± 0.2

3. Results and discussion

To evaluate the distribution of chitosan onto and within the paper sheet, it was essential to establish that papers coated with the *same amount* of either CH or FITC–CH (Table 1) would give properties which were not affected by the presence of the fluorescent substituents on the macromolecules, except of course for the features purposely associated with the introduction of these moieties. In order to assess this point, we first compared the air permeability of differently coated sheets and verified that the changes in this property as a function of the number of deposited layers was the same for both chitosans used, as shown Table 1. The second comparison consisted in measuring the tensile index of these coated sheets and, as clearly suggested by the data given in Table 2, the two chitosans induced the same quantitative effects within experimental error. The actual variations in these two properties will be discussed in a forthcoming publication together with the effect of other parameters.

3.1. Evaluation of the distribution of chitosan onto the paper sheets

Three different approaches were applied to assess how the coated macromolecules had distributed themselves both on the sheet surface and in its depth.

3.1.1. Reflectance

To gain some understanding of the role of the presence of chitosan layers in terms of its penetration within the paper sheet, visible diffuse reflectance measurements were carried out on both sides (coated and uncoated) of the FITC–CH-coated papers bearing up to five different layers. We measured the same reflectance spectrum between 400 and 600 nm for all the paper sheets, both at their CS coated and uncoated sides, using two random pieces cut out of each sheet. The CS remission function (with an intensity lower than 0.01 between 420 and 570 nm) was deduced from all the spectra of the coated paper sheets. Fig. 1 clearly shows a saturation of the intensity of the reflectance signal after the third layer on both sides of the paper. Fig. 2 displays a linear increase in the Kubelka–Munk function at 507 nm for the first three layers, followed by its stabilization for the two additional ones, suggesting that chitosan had attained a complete surface coverage and hence a constant reflectance intensity. This hypothesis was confirmed by the similar variation of the maximum wavelength intensity with the number of layers for the coated and uncoated paper sheets shown in Fig. 1.

The variation of reflectance (in the range of 503–508 nm) for the first three is related to the interaction of chitosan with the paper components (mainly cellulose fibers), which induced a modification of the environment of the chitosan derivative and a shift in the absorption wavelength. For the fourth and fifth layers, the wavelength maximum stayed at 508 nm, given the fact that the coverage of the paper surface reached completion.

The fact that the fluorescent chitosan derivative was also detected on the *uncoated* side of the sheets confirmed that it penetrated progressively throughout the paper thickness all the way to the other side.

3.1.2. Luminescence

Fig. 3A compares the emission features of the uncoated and coated paper sheets under UV excitation. For all of them, the spectra displayed a main broad band with two components peaking around 430 nm, attributed to the optical brighteners agents present in the paper sheets. For the FITC–CH-coated sheets, an addi-

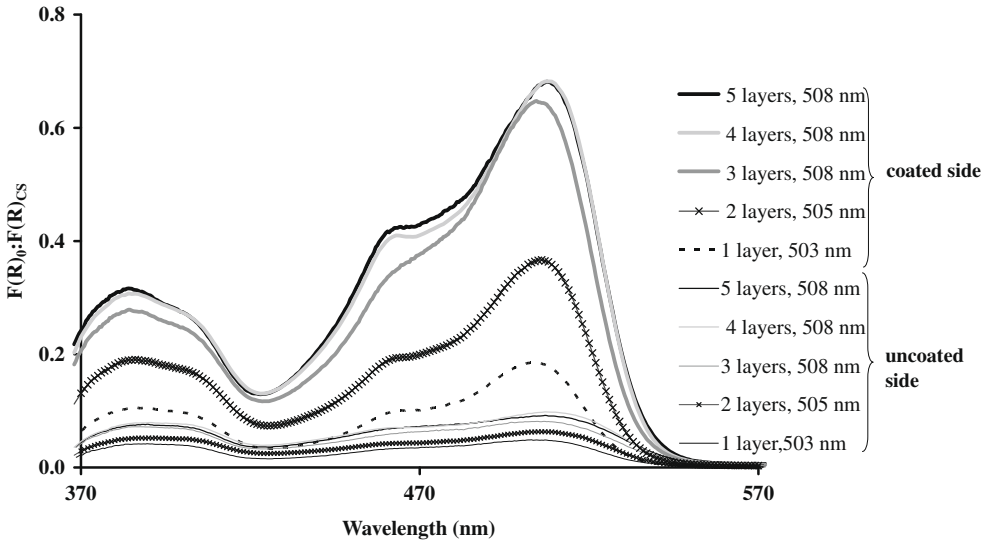

Fig. 1. Visible diffuse reflectance spectra of coated and uncoated side of FITC–CH-coated paper for one to five chitosan layers.

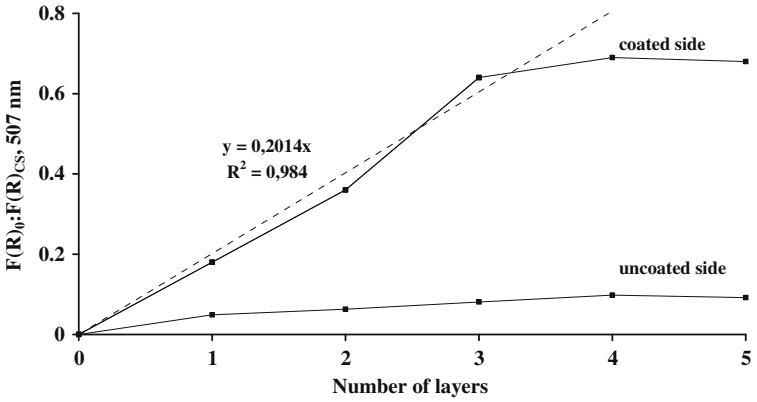

Fig. 2. Intensity variation at 507 nm of the remission function for the coated and uncoated side of FITC–CH-coated paper with the number of chitosan layers.

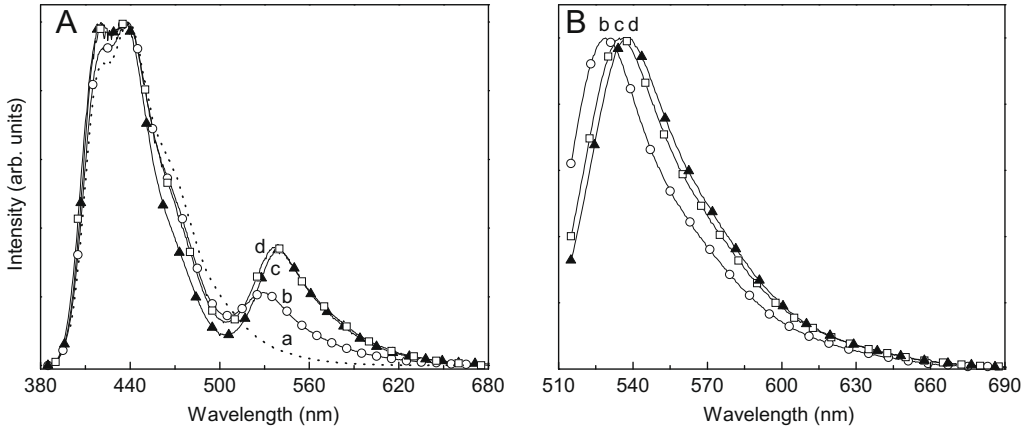

Fig. 3. Emission spectra of the CS (a, dotted line) and of the FITC–CH1 (b, open circles), FITC–CH3 (c, solid triangles) and FITC–CH5 (d, open squares) sheets excited at (A) 370 nm and (B) 500 nm.

tional emission band peaking at higher wavelengths was detected. This coating-related emission was in tune with that of the fluorescein moiety, known to occur around 510–540 nm (Guan et al., 2007). Increasing the excitation wavelength from 350 to 500 nm (Fig. 3B), no change in the energy of the emission bands was measured, but only an enhancement in the relative intensity of the high-wavelength component. As the number of FITC–CH deposited layers increased from 1 to 5, the fluorescein-related emission exhibited a bathochromic shift from 531 nm to 538 nm (Figs 3A and B), attributed to the increase in the fluorescein concentration, as already observed for other dye compounds (Anedda et al., 2005; Canham, 1993).

The effect of the coating on the emission features of the paper sheet under UV/Vis excitation was quantified through the estimation of the CIE (x,y) colour coordinates. Fig. 4 shows the chromaticity diagram for the emission colour of the CS as well as the FITC–CH1 and FITC–CH3 sheets under two selected excitation wavelengths. The colour coordinates of the FITC–CH5 paper were omitted because they resembled those of the FITC–CH3 homologue. The emission colour coordinates of the CS were independent of the excitation wavelength and located in the purplish-blue region of the diagram. Under UV excitation, the emission colour coordinates of the FITC–CH samples deviated towards the centre of the diagram due to the contribution of the chitosan-related emission component (Fig. 3). Under visible excitation, the emission colour coordinates were close to pure colours within the green region. By controlling the number of deposited layers and by

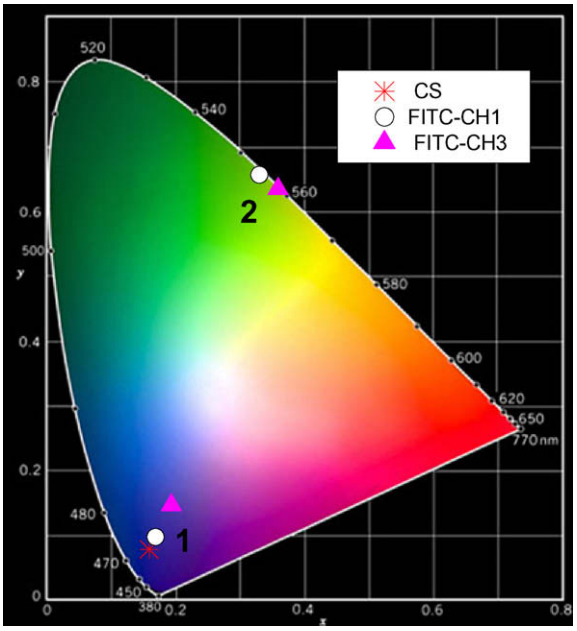

Fig. 4. CIE chromaticity diagram (1931) showing the emission colour coordinates of the CS as well as of the FITC–CH1 and FITC–CH3 excited at (1) 370 nm and (2) 500 nm (For interpretation of color mentioned in this figure legend the reader is referred to the web version of the article.).

varying the excitation wavelength from 370 nm to 500 nm, the emission colour coordinates could be readily tuned from the purplish-blue (FITC–CH1, (0.19,0.09)) to the bluish-purple (FITC–CH3, (0.20,0.14)) regions and from the yellowish-green (FITC–CH1, (0.33,0.65)) to the yellow–green (FITC–CH3, (0.36,0.63)) spectral regions, respectively.

The emission properties of the coated paper sheets were further quantified by the measurement of the radiance under UV/Vis excitation (370 and 500 nm). The average values found for FITC–CH1, FITC–CH3 and FITC–CH5 were 0.040, 0.029, and 0.027 $\mu W\ cm^{-2}sr^{-1}$ at 370 nm and 3.471, 4.465 and 5.311 $\mu W\ cm^{-2}sr^{-1}$ at 500 nm, respectively. Using the 370 nm excitation, the highest radiance value for the FITC–CH1 was due to the higher relative contribution of the uncoated paper intrinsic emission to the overall photoluminescence features. Increasing the number of coating layers from 1 to 3 to 5, the radiance values decreased, indicating a more efficient coating. The similarity between the radiance values for FITC–CH3 and FITC–CH5 suggests that beyond three layers, a saturation of the paper coating was attained, as the diffuse reflectance spectra pointed out. By exciting selectively the FITC–CH-related emission, the radiance values increased progressively (up to 20–30%) with the number of deposited layers, indicating a higher contribution of the FITC–CH centres for the luminescence features. For both excitation wavelengths, the standard deviation was within the experimental error, confirming a homogeneous distribution of the deposited fluorescent chitosan.

3.1.3. Morphological properties

The morphology of the CS and FITC–CH papers was investigated by SEM using different magnifications (150×, 500× and 1500×) and views (coated side, uncoated side and cross-section). The SEM images of the FITC–CH-coated papers (Fig. 5–7) clearly showed the features of their three major components, viz. the fibers, the inorganic fillers and the chitosan film, the latter being

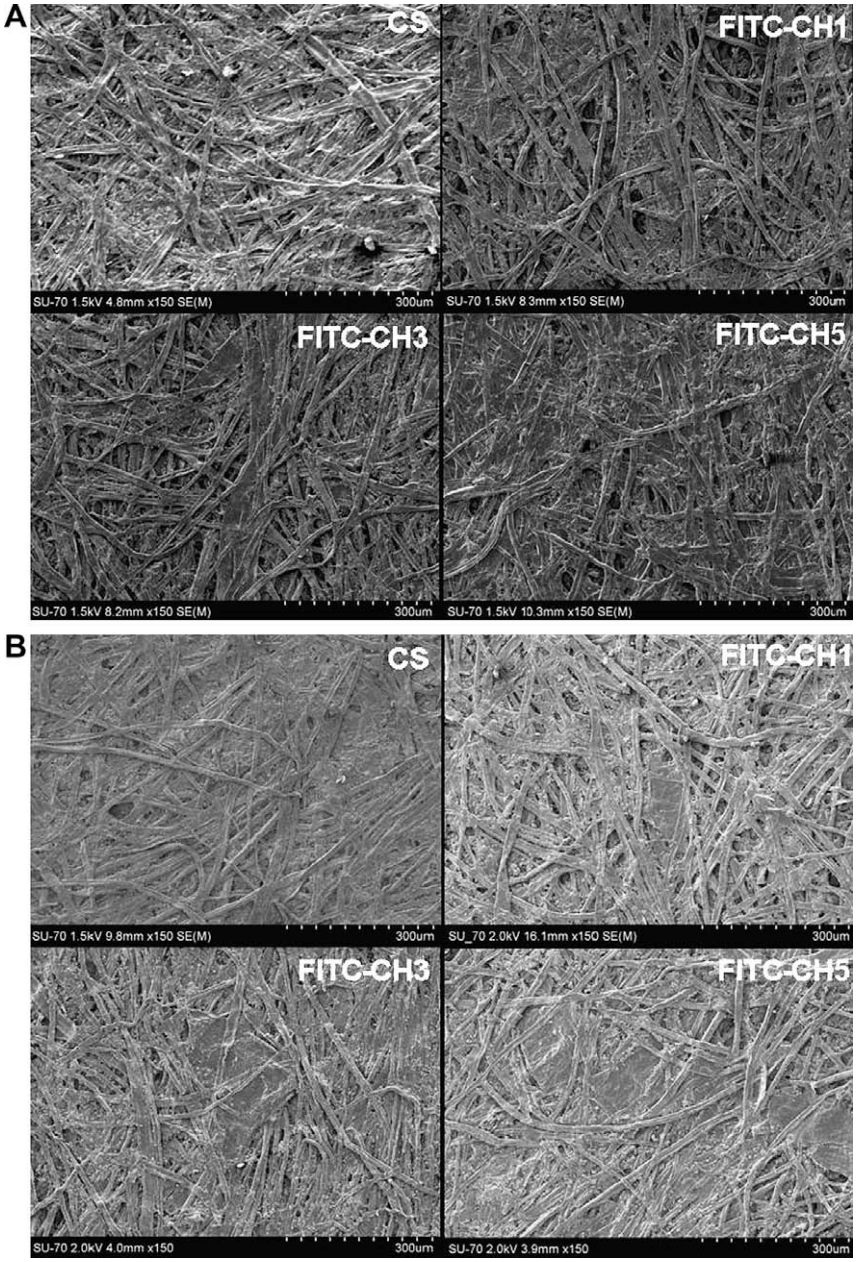

Fig. 5. SEM surface views (150×) of the CS, FITC–CH1, FITC–CH3 and FITC–CH5-coated paper from the coated (A) and uncoated sides (B).

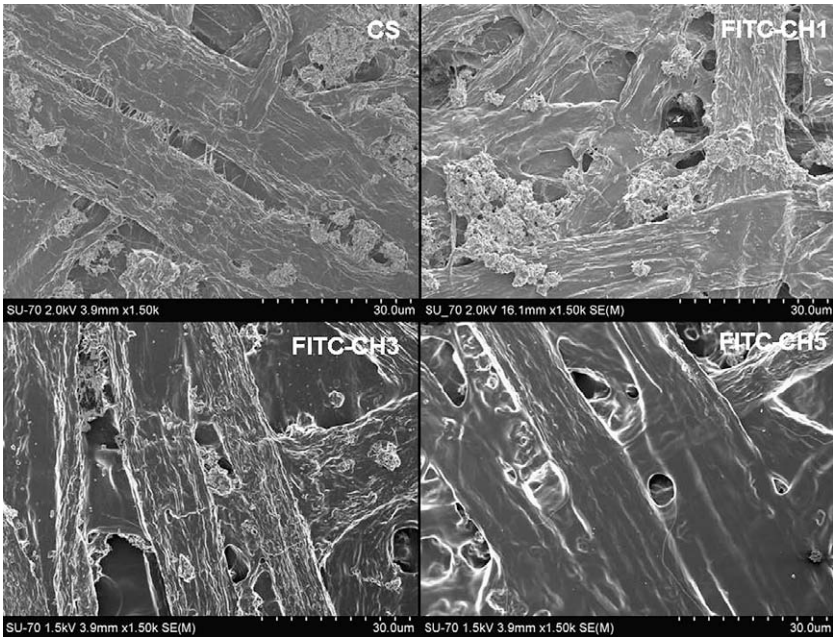

Fig. 6. SEM surface views (1500×) of the CS, FITC–CH1, FITC–CH3 and FITC–CH5-coated paper from the coated side.

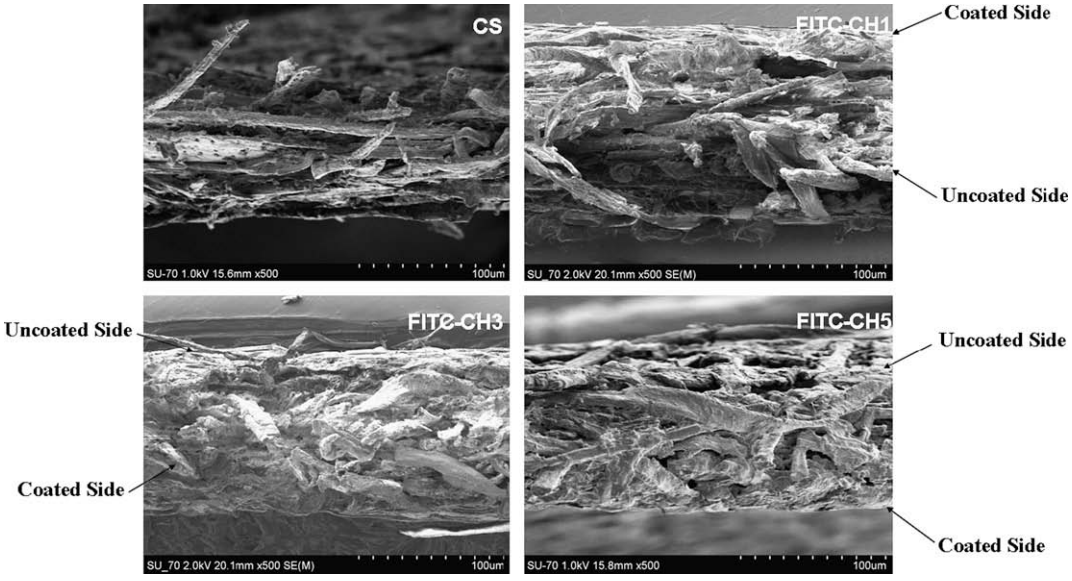

Fig. 7. Microscopic cross-sectional views (500×) of the CS, FITC–CH, FITC–CH3 and FITC–CH5-coated paper.

particularly evident when three or more CH layers were applied. The most interesting feature, however, has to do with the uniformity of the chitosan film over all the examined surfaces, which corroborates the spectroscopic observations.

However, although the surface of fibers was completely CH-coated when three or more layers were applied, the polymer did not fill completely the paper pores on its 3D structure, even with the five layers. The presence of chitosan on the back of the sheet, shown in Fig. 5B, confirms that this polymer did penetrate through the fiber network. As expected, this effect was strongly dependent on the number of deposited chitosan layers, particularly for the first three applications.

The information provided by the images obtained at higher magnifications (Fig. 6) was particularly instructive because it showed that as the number of chitosan layers increased, its well-known film-forming aptitude achieved a progressively more continuous morphology leading to a smooth surface coverage which incorporated both fibers and fillers. Particularly visible in these micrographs is the growing evenness of the sheet surface, as the thickness of the added polymer increases, which of course is a major feature in terms of the decrease in surface roughness (rugosity) and hence, most probably, of improved printing quality.

The observation of the cross-section images (Fig. 7), revealed a progressive compaction of the fibers under the influence of a growing number of chitosan layers, a "gluing" effect which confirmed that the polymer did indeed penetrate within the paper sheet, to an extent that obviously depended on the number of its successive additions. This intimate interaction between two polysaccharides is not surprising, given their structural affinity which translates into a pronounced tendency to form intermolecular hydrogen bonds.

4. Conclusion

With this study we found that the distribution of chitosan onto the chitosan-coated paper is uniform and that this macromolecule does not have a preferential way to cover the surface of the paper. Chitosan penetration into the sheets occurs progressively with the first layers and after a supplementary coating onto the paper sheet is observed. Both reflectance and luminescence, showed a saturation of the FITC–CH-coated paper after the three layers. The experimental approach presented here to assess chitosan distribution on chitosan-coated paper may be certainly extrapolated to the study of other paper-coating agents.

Acknowdgements

The authors thank Norwegian Chitosan AS. (Norway) for their generous gift of chitosan. Thanks also to RAIZ – Centro de Investigação da Floresta e do Papel for the paper sheets and the use of their equipments and their collaboration and assistance. Susana Fernandes thanks the Fundação para a Ciência e a Tecnologia (Portugal) for a Scientific Research grant (SFRH/BD/41388/2007).

References

Anedda, A., Carbonaro, C. M., Clemente, F., Corpino, R., Grandi, S., Magistris, A., et al. (2005). Rhodamine 6G–SiO_2 hybrids: A photoluminescence study. *Journal of Non-Crystalline Solids, 351*, 1850.

Bordenave, N., Grelier, S., Pichanvant, F., & Coma, V. (2007). Water and moisture susceptibility of chitosan and paper-based materials: Structure-property relationships. *Journal of Agriculture and. Food Chemistry, 55*, 9479–9488.

Canham, L. T. (1993). Laser dye impregnation of oxidized porous silicon on silicon wafers. *Applied Physics Letters, 63*, 337.

Fang, Y., Ning, G., Hu, D., & Lu, J. (2000). Synthesis and solvent-sensitive fluorescence properties of a novel surface-functionalized chitosan film: Potential materials for reversible information storage. *Journal of Photochemistry and Photobiology A: Chemistry, 135*, 141–145.

Gällstedt, M., Brottman, A., & Hedenqvist, M. (2005). Packaging-related properties of protein-and chitosan-coated paper. *Packaging Technology & Science, 18*, 161–170.

Gåserød, O., Smidsrød, O., & Skjåk-Bræk, G. (1998). Microcapsules of alginate–chitosan - I A quantitative study of the interaction between alginate and chitosan. *Biomaterials, 19*, 1815–1825.

Guan, X., Liu, X., & Su, Z. (2007). Rhodamine-conjugated acrylamide polymers exhibiting selective fluorescence enhancement at specific temperature ranges. *Journal of Applied Polymer Science, 104*, 3960–3966.

Kjellgren, H., Gällstedt, M., Engström, G., & Järnström, L. (2006). Barrier and surface properties of chitosan-coated greaseproof paper. *Carbohydrate Polymers, 65*, 453–460.

Kubelka, P., & Munk, P. Z. (1931). Optics of coloring. *Technical Physics, 12*, 593–601.

Kuusipalo, J., Kaunisto, M., Laine, A., & Kellomäk, M. (2005). Chitosan as a coating additive in paper and paperboard. *Tappi Journal, 4*(8), 17–21.

Li, H., Du, Y., & Xu, Y. (2004). Adsorption and complexation of chitosan wet-end additives in papermaking systems. *Journal of Applied Polymer Science, 91*, 2642–2648.

Peniche, C., Argüelles-Monal, W., & Goycoolea, F. M. (2008). Chitin and chitosan: Major sources, properties and applications. In M. Belgacem & A. Gandini (Eds.). *Polymers and composites from renewable resources* (Vol. 25, pp. 517–542). Amsterdam: Elsevier [and references therein].

Qaqish, R. B., & Amiji, M. M. (1999). Synthesis of a fluorescent chitosan derivative and its application for the study of chitosan–mucin interactions. *Carbohydrate. Polymers, 38*, 99–107.

Rinaudo, M., Milas, M., & Dung, L. P. (1993). Characterization of chitosan. Influence of ionic strength and degree of acetylation on chain expansion. *International Journal of Biological Macromolecules, 15*, 281–285.

Tømmeraas, K., Strand, S. P., Tian, W., Kenne, L., & Vårum, K. M. (2001). Preparation and characterisation of fluorescent chitosans using 9-anthraldehyde as fluorophore. *Carbohydrate Research, 336*, 291–296.

Vartiainen, J., Motion, R., Kulonen, H., Rättö, M., Skyttä, E., & Ahvenainen, R. (2004). Chitosan-coated paper: Effects of nisin and different acids on the antimicrobial activity. *Journal of Applied Polymer Science, 94*, 986–993.